JOURNAL OF MATERIALS SCIENCE 19 (1984) 607–614

Significance of limiting (equivalent) tip radius and crack tip deformation for cleavage induced fracture in structural steels

R. K. PANDEY
Department of Applied Mechanics, Indian Institute of Technology, Delhi 110016, India

In two structural steels, the limiting crack tip radius (LTR) and the crack tip blunting radius have been evaluated at the instant of fracture initiation by cleavage. The effect of yield strength on LTR and the blunting radius has been investigated. The relationship between the limiting and the blunting tip radius has been studied. The limiting tip radius has been found to be of the order of the plastic zone radius in the structural steels investigated.

1. Introduction

Sharp fatigue cracks are recommended in the fracture toughness (FT) specimens for measurement of a meaningful fracture toughness value. The fracture toughness has been found to increase with increasing radius of the crack [1, 2]. Thus a most conservative estimate of fracture toughness value can be obtained by using a sharp crack in the specimens. It has been reported, however, that the toughness value attains a minimum level for a finite tip radius and a further decrease in crack tip radius does not influence the value of fracture toughness [3, 4]. Thus, a correct value of fracture toughness can also be obtained from a specimen provided with a notch of finite radius rather than a fatigue crack if the notch tip radius is within the limit of the critical value of radius. The critical value of tip radius, up to which the fracture toughness remains constant and increases only when the tip radius is exceeded, is termed as the limiting tip radius (LTR) in this investigation. It is of great interest to know what type of defects, present in engineering structures and components, can behave like sharp cracks. Also, the extent to which the stringent requirement of a sharp fatigue crack in fracture toughness testing can be relaxed, is a valuable piece of information. The knowledge of the limiting tip radius of a material can provide answers to these questions.

The present investigation has been conducted with the above objective in mind. The significance of LTR has been studied in structural steels for cleavage induced fracture. It may be noted that LTR in the present investigation has not been evaluated by varying the radius of the actual crack. Instead, a limiting equivalent tip radius has been obtained by testing precracked specimens and using existing theories for cleavage induced fracture. An attempt has been made to compare the LTR with the crack tip blunting radius at the instant of fracture initiation. By changing the test temperature and loading rate in structural steels, the yield strength has been changed and cleavage fracture has been obtained at different yield strength levels. The effect of yield strength on LTR has been investigated. The role of the microstructure and plastic zone size, etc. *vis-à-vis* the limiting tip radius, has been discussed.

2. Materials and experimental determination of blunting tip radius

2.1. Materials

The investigation has been conducted in two structural steels, the compositions and tensile properties of which are given in Table I. Steel A is a Lloyd's grade mild steel used in ship-building whereas steel B is a HSLA type, where the addition of vanadium has been made to refine the

0022–2461/84 $03.00 + .12

TABLE I Chemical composition and tensile properties of steels

Steel samples	Composition						Yield strength (MPa)	Tensile strength (MPa)	% elongation
	C	Mn	Si	P	S	V			
A	0.16	0.80	0.03	0.009	0.19	–	245	420	40
B	0.20	1.60	0.235	0.032	0.027	0.12	465	630	36

grain diameter and cause finer dispersion of vanadium carbides within the grains of ferrite. The typical grain diameter of ferrite is 27 and 18 μm, respectively, in steels A and B. The tensile properties of the alloys can be radically changed by changing the test temperature and the loading rate without affecting the microstructure. The mechanism of fracture initiation changes from cleavage, quasi-cleavage at low temperature – high strain rate regime to microvoid coalescence at increased temperature – low strain rate regime. Thus, the alloys provide a wide region over which to study the significance of crack tip deformation and limiting radius for a given micromechanism of fracture without causing any disturbance to the microstructure.

2.2. Tensile test

The round tensile specimens of diameter 4.5 mm and gauge length 16 mm were tested on an Instron machine at temperatures 77, 178, 196 and 300 K with crosshead speeds ranging from 0.05 to 50 mm min^{-1}. The tensile properties were evaluated from the load–elongation diagrams. The temperature dependence of yield strength for three strain rates, i.e. 10^{-5}, 10^{-3} and 10^{0} sec^{-1} is shown in Fig. 1 for alloys A and B.

2.3. Determination of blunting crack tip radius

From the analysis of the slip line field near the crack tip, Rice and Johnson [5] have studied the associated crack tip deformation under plane

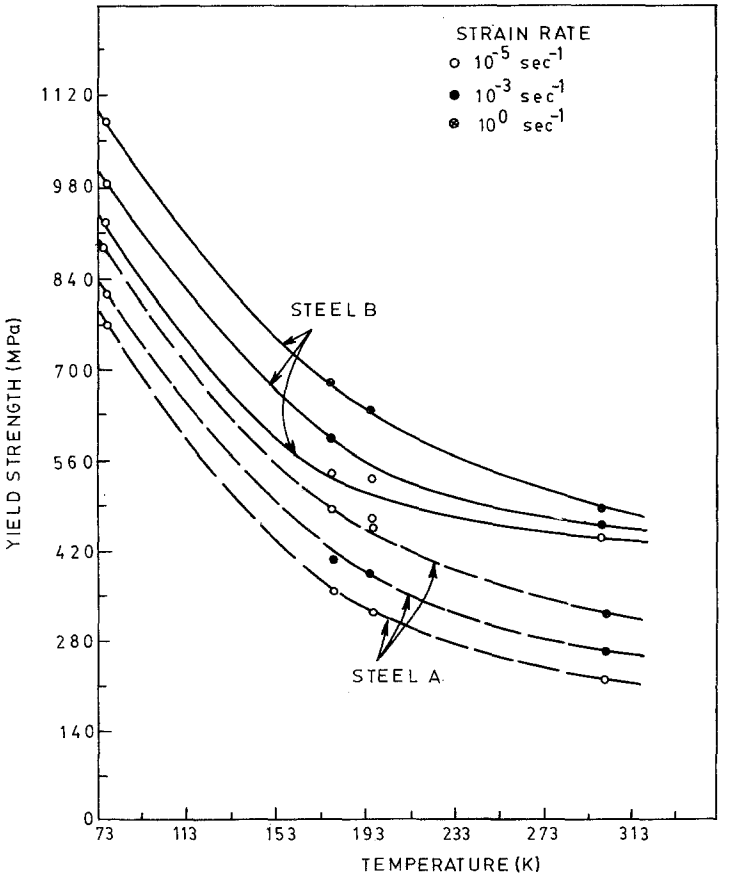

Figure 1 Temperature dependence of yield strength for $\dot{\epsilon}_c = 10^{-5}$, 10^{-3}, 10^{0} sec^{-1}.

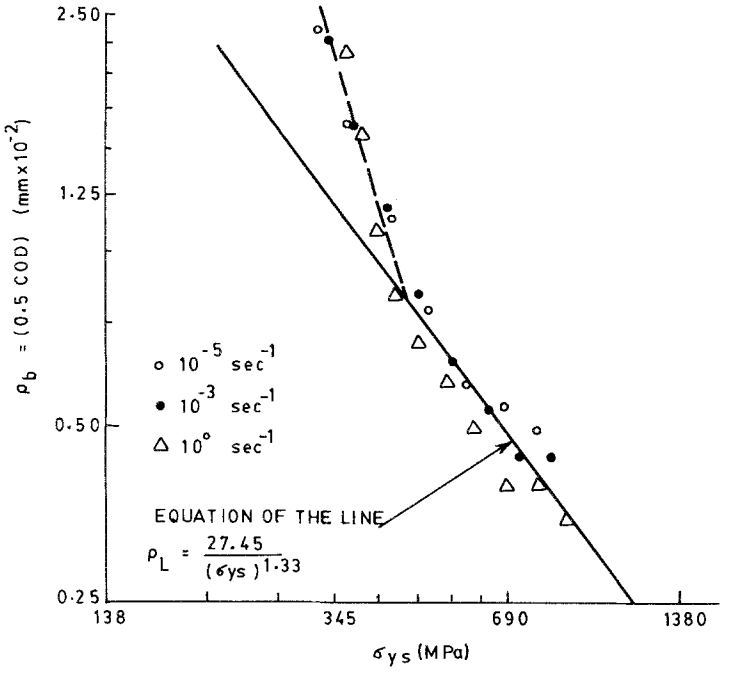

Figure 2 Blunting crack tip radius as a function of σ_{ys} in steel A.

strain conditions. It is believed that the deformed crack tip assumes a semicircular shape. The SEM examination of fracture surfaces in the FT specimens has revealed considerable stretching of the crack tip [6, 7]. The extent of stretching increases with the K_{Ic}/σ_{ys} ratio of the material. The width of the stretched zone has been observed to be in the range of 0.5 (CTOD) in plane strain condition [6], where CTOD is the crack tip opening displacement. This is in agreement with the semicircular shape of a deformed crack as envisaged by Rice and Johnson [5]. Thus the radius of the deformed crack tip at the instant of crack initiation or fracture can be obtained from the measured CTOD values.

The CTOD values were obtained by testing SEN bend specimens of dimensions 12.5 mm (thickness) × 12 to 15 mm (width) × 80 mm (span length) provided with sharp fatigue cracks. The specimens were loaded in a 2.5 ton screw-driven machine under three-point bending. The mouth opening displacement, V, was measured using a displacement gauge. The CTOD values were evaluated from the mouth opening displacement corresponding to a crack initiation point (as discussed later in Section 3.1) using the relationship [8],

$$\text{CTOD} = \frac{V}{1 + n\left(\frac{a+z}{W-a}\right)} \quad (1)$$

where a is the crack length, W is the width, z is the distance of the clip gauge from the test piece surface, and n is a constant giving the position of the rotation axis from the crack tip. The values of n were determined as given in [9]. The CTOD values were obtained at temperatures 77, 133, 178, 196, 255, 300 K and at crosshead speeds of 1 to 200 mm min^{-1}. The blunting crack tip radii ρ_b at different test temperatures were obtained using the relation:

$$\rho_b = \frac{\text{CTOD}}{2} \quad (2)$$

As the test temperature decreases or rate of straining increases, the CTOD value decreases and the value of ρ_b decreases consequently. The variation of ρ_b as a function of yield strength is shown in Fig. 2 for steel A. An identical nature was observed for steel B also, and therefore it has not been reported.

3. Evaluation of limiting crack tip radius

The LCTR (ρ_L) is defined as the maximum radius of a notch or crack which can provide a ρ independent toughness value. A further increase in radius beyond the limiting crack tip radius increases the value of fracture toughness. Using the slip line field analysis and elastic–plastic stress distribution in the notched bars, a criterion for cleavage fracture was given [3, 10] which is based on the fact that the unstable fracture occurs when the plastic zone spreads to a critical distance such that the maximum tensile stress level in the plastic

zone is raised from the yield strength to the cleavage fracture strength over a small volume in front of the notch. The toughness, K_{Ic} is expressed in terms of the microscopic cleavage strength, σ_f^* and the tensile yield strength σ_{ys} as [10],

$$K_{Ic} = 2.89\,\sigma_{ys}\left(\exp\left(\frac{\sigma_f^*}{\sigma_{ys}} - 1\right) - 1\right)^{1/2}(\rho_0)^{1/2} \quad (3)$$

where ρ_0 is defined as critical value of root radius below which K_{Ic} is independent of root radius ρ and achieves its minimum value. Thus ρ_0 is the same as the limiting crack tip radius, ρ_L.

In the present investigation the ρ_L values were determined from Equation 3 at different test temperatures and thus at different yield strength levels. This was done by evaluating the toughness parameter and the cleavage fracture strength, σ_f^*, as given below.

3.1. Determination of toughness parameter

A fracture criterion based on the stress intensity factor (K) is not applicable at all the test temperatures in the steels under investigation. In view of the limited applicability of LEFM, i.e. only in the regime of low temperature–high strain rate, it was decided to use J_{Ic} toughness parameter for the sake of consistency in the entire spectrum of loading conditions. The equivalent K_{Ic} values, K_{Ic}^J, can be obtained by using the relationship

$$J_{Ic} = (1-\nu^2)\frac{(K_{Ic}^J)^2}{E} \quad (4)$$

where ν is the Poisson's ratio and E is the Young's modulus. J_{Ic} measurement was made on precracked SEN specimens under three point bend loading (as described for CTOD determination). The tentative value of J, J_Q was obtained using [11],

$$J_Q = \frac{2A}{B(W-a)} \quad (5)$$

where A is the area under a load–load point deflection (L–D) curve up to the point of crack initiation. In the low temperature–high strain rate regime of testing where the LEFM could be applied as well, the crack initiation point was given by the maximum load point or 5% secant line. However, in high temperature–low strain rate regime of testing, the 5% secant or maximum load point could no longer be used to obtain the crack initiation point. At the maximum load point the crack growth was found to be of the order of 15 to 21% of the original crack length. The crack initiation point was detected by dividing the L–D plot into various regions and identifying the stage where rapid increase in compliance (i.e. compliance jump) was noted. This point represents the crack initiation point in these specimens [12]. The validity of J_Q for J_{Ic} was tested as per the condition [13, 14];

$$a, B, (W-a) \geqslant 25\frac{J_Q}{\sigma_{ys}} \quad (6)$$

The variation of J_{Ic}/J_Q (as obtained in this investigation) with yield strength is shown in Fig. 3. The equivalent K_{Ic}^J values were calculated from Equation 4. Fig. 4 shows the variation of K_{Ic}^J value as a function of test temperature for three strain rates.

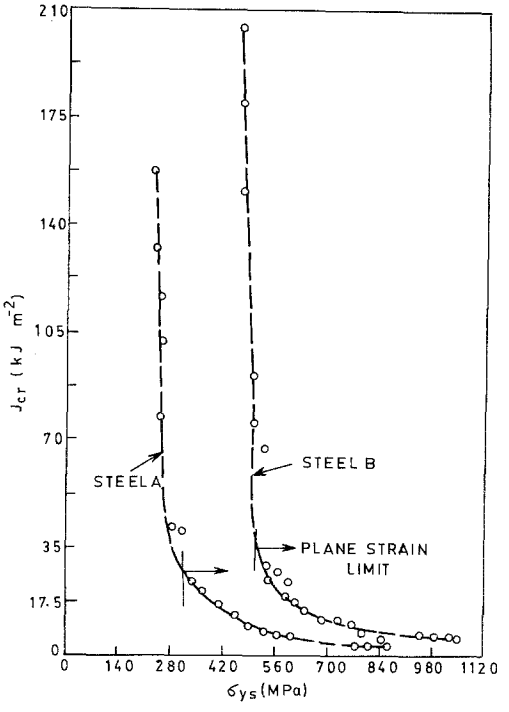

Figure 3 Yield strength dependence of J_{cr} for steels A and B.

3.2. Determination of cleavage fracture strength, σ_f^*

σ_f^* values were determined from the σ_{ys} value at temperature T^* where T^* is the temperature at which the ratio P_f/P_{gy} (fracture load/general yield load) is 0.8 [10]. The yield load values P_y at different temperatures were obtained from tensile yield strength values at corresponding temperatures using the relation for three point bending [15],

$$M = \left(\frac{\sigma_{ys}}{4}\right)(W-a)^2B = \frac{P_yS}{4} \quad (7)$$

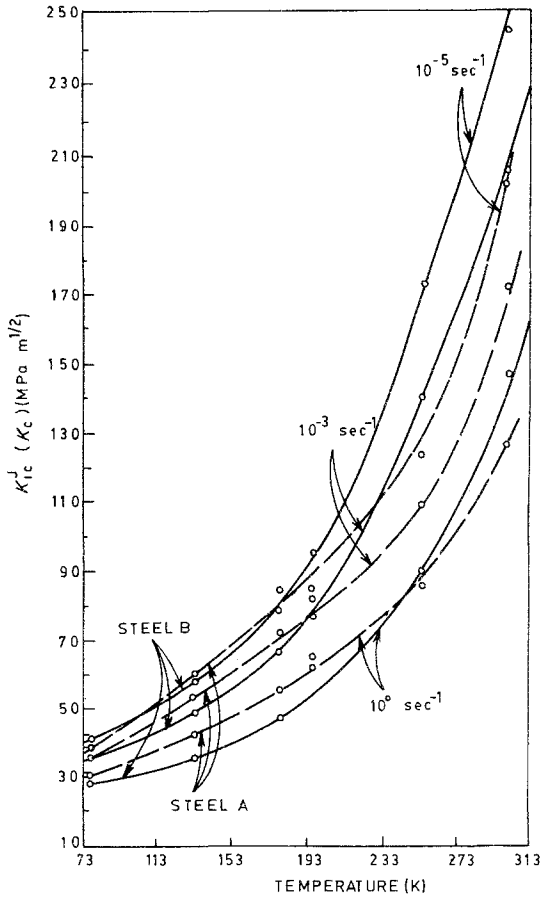

Figure 4 Temperature variation of K^J_{Ic} (K_c) for $\dot{\epsilon}_c = 10^{-5}$, 10^{-3}, 10° sec^{-1}.

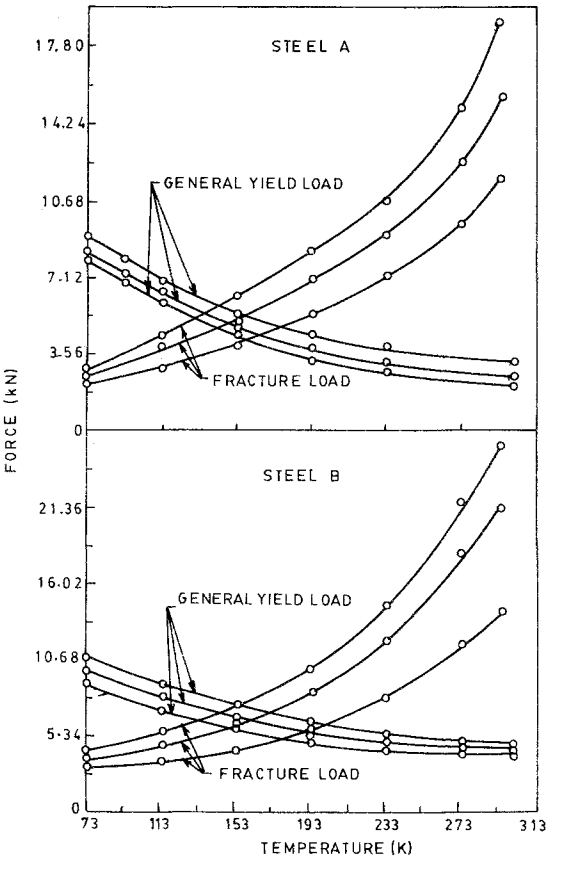

Figure 5 Fracture load and general yield load against temperature in three point bend specimens with dimensions 12.5 × 12.5 × 62.5 mm, crack length 12.5 mm.

where M is the applied bending moment and S is the span length. Using a constraint factor, L, of 1.26 the general yield load, P_{gy} was computed from P_y [15]. The experimentally obtained fracture loads for three point bending, P_f, were used. The plot of general yield load and fracture load against temperature is shown in Fig. 5 for strain rates 10^{-5}, 10^{-3} and 10° sec^{-1}, σ^*_f can be expressed as [15, 16],

$$\sigma^*_f = \left(1 + \frac{\pi}{2} - \frac{\omega}{2}\right) \sigma_{ys\ (evaluated\ at\ T^*)} \quad (8)$$

where ω is the flank angle of the notch and taken to be zero for the crack. The values of σ^*_f, etc., are shown in Table II. With increasing strain rate a mild decrease in σ^*_f is noted from the table.

3.3. Computation of limiting crack tip radius

Substituting the values of cleavage fracture strength σ^*_f, K^J_{Ic} and σ_{ys} in Equation 3, the ρ_L values were calculated at different temperatures. The ρ_L values are plotted against the yield strength in Fig. 6 for the alloys A and B.

TABLE II Determination of cleavage fracture strength

Strain rate, $\dot{\epsilon}$ (sec^{-1})	Steel A			Steel B		
	$T_{D(N)}$(K)	T^*(K)	σ^*_fMPa)	$T_{D(N)}$(K)	T^*(K)	σ^*_f(MPa)
10^{-5}	130	117	1463	137	119	1928
10^{-3}	147	131	1449	161	141	1828
10°	178	161	1332	202	183	1684

$T_{D(N)}$ is the temperature corresponding to the point of intersection of P_f and P_{gy} curves.

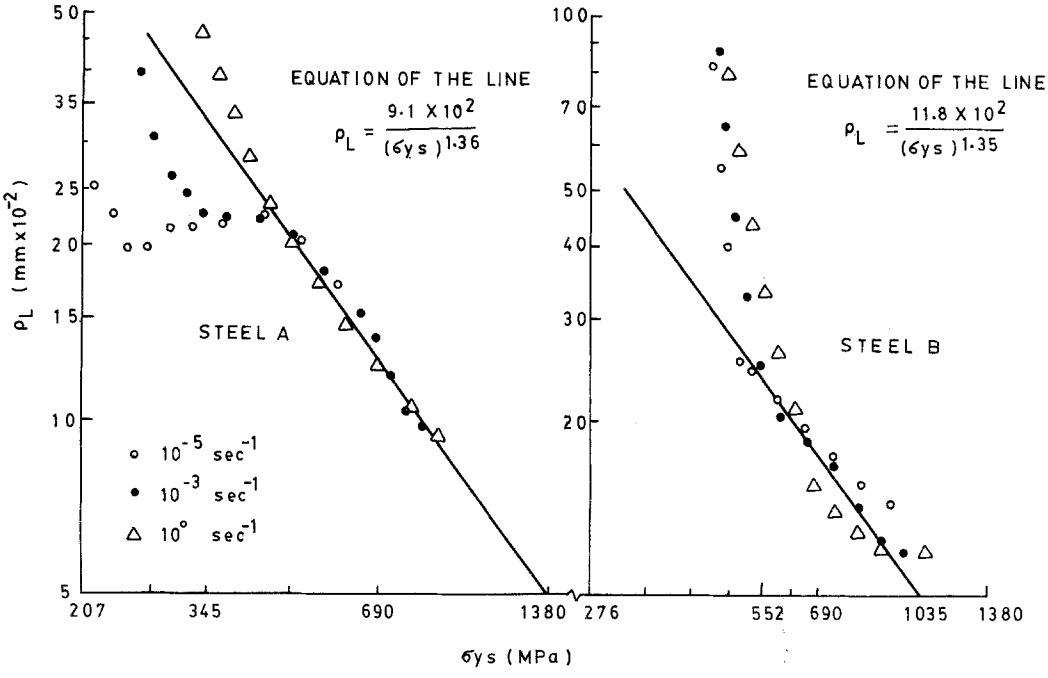

Figure 6 LTR as a function of σ_{ys}.

4. Discussion

4.1. Dependence of blunting crack tip radius on yield strength

It may be noted from Fig. 2 that as the yield strength increases, the blunting associated with the crack at the instant of fracture intiation decreases. The relationship between the blunted radius of the crack and the yield strength can be given by the following expression in steel A

$$\rho_b = \frac{27.45}{(\sigma_{ys})^{1.33}} \quad (9)$$

It may be appreciated that the above equation is valid only in the regime of temperature, etc., where the initiation of fracture occurs by the cleavage mechanism. The minimum yield strength at which fracture by the cleavage mechanism is expected is around 415 MPa as can be seen from the figure. It was noted from the SEM examinations of fracture surfaces in alloys A and B that up to 178 K temperature and below, the fracture initiation is fully by cleavage mode in both the alloys. At 196 K, the cleavage is found to be mixed with dimples in a smaller proportion. The corresponding yield strength at 196 K are around 448 MPa and 634 MPa in steels A and B, respectively. Thus for 415 MPa yield strength in steel A, the cleavage mode is not without the presence of microvoid coalescence. The blunting crack tip radius is observed to be larger for the fibrous (microvoid coalescence) mechanism of fracture as compared to that of the cleavage mechanism for the same yield strength level. In other words, the minimum volume of material to be strained at the crack tip for the initiation of fracture by cleavage is smaller than the same for microvoid coalsescence mode for a given microstructure of material.

4.2. Limiting crack tip radius as a function of yield strength

From Figs. 6a and b the relationship between ρ_L and σ_{ys} is evident. This can be expressed as

$$\rho_L = \frac{9.1 \times 10^2}{(\sigma_{ys})^{1.36}} \quad \text{(for steel A)} \quad (10)$$

$$\rho_L = \frac{11.8 \times 10^2}{(\sigma_{ys})^{1.35}} \quad \text{(for steel B)} \quad (11)$$

for cleavage induced fracture. A linear relationship exists between ρ_L and σ_{ys} on log–log scale for cleavage fracture. The expected yield strength level for cleavage fracture from Figs. 6a and b are around 420 MPa and above for steel A and 560 MPa and above for steel B. At lower yield strength where fibrous initiation begins in preference of cleavage, the relation between ρ_L and σ_{ys} is uncertain (Fig. 6a). One reason for this uncertainty is the inapplicability of Equation 3 for fibrous initiation of fracture.

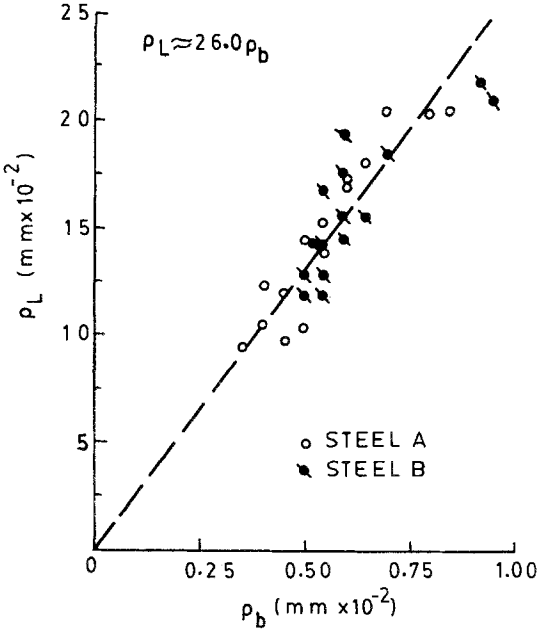

Figure 7 Relation between ρ_b and ρ_L in stress induced fracture range (cleavage fracture).

4.3. Relationship between blunting crack tip radius and the limiting crack tip radius

It is of interest to see how the limiting crack tip radius ρ_L varies with the blunting crack tip radius ρ_b. This is shown in Fig. 7 for the regime of cleavage fracture. The blunting tip radius appears to be linearly related with the LTR as may be seen from the figure. An approximate relation between the two may be given as

$$\rho_L = 26.0 \rho_b \tag{12}$$

It is significant to note that Equation 12 is applicable for both the alloys. Thus, ρ_L and ρ_b seem to be uniquely related in steels A and B in spite of their differences in grain size and inclusion content. The grain size does not appear to control the limiting crack tip radius. This is contrary to the earlier belief [14] that the microstructural features like grain size or inclusion spacing determine the effective limiting sharpness. Moreover, the value of LTR for cleavage induced fracture lies in the range of 100 to 200 μm as can be seen from Fig. 7. This is 5 to 10 times larger than the ferrite grain diameter and expected to be much larger than the average inclusion spacing.

4.4. Limiting crack tip radius as compared with plastic zone radius

For the initiation of fracture from a sharp crack, a critical size of plastic zone has to develop at the crack tip. The microscopic process of fracture is confined in the (critical) plastic zone [3, 17]. Even in presence of a very sharp crack, the straining over a critical length (and thus over a critical volume) is a must to initiate the microfracture process [18] (e.g. blocking of glide bands by an obstacle-like grain boundary, twin boundary, etc., and the cleavage crack formation due to stress concentration at microscopic level). It is contented that as long as the radius of crack tip is smaller than the critical plastic zone radius it does not influence the process of crack initiation. Once the tip radius crosses the radius of critical plastic zone, the effect of crack radius gets reflected on the energy for fracture initiation and ρ dependent fracture toughness value is obtained. Thus, an intimate relationship between the critical plastic zone radius, R_c (i.e. the plastic zone radius at the instant of fracture in presence of a sharp crack) and the LTR, ρ_L is expected. An attempt was made to compare the R_c with the ρ_L value in the present work. The R_c values were obtained using Irwin–McClintock's model [19],

$$R_c = \frac{1}{6\pi}\left(\frac{K_{Ic}}{\sigma_{ys}}\right)^2 \tag{13}$$

TABLE III Comparison of plastic zone radius with the LTR for cleavage fracture

Steel A				Steel B			
σ_{ys} (MPa)	K_{Ic}^J (MPa m$^{1/2}$)	Critical plastic zone radius (mm)	LTR (mm)	σ_{ys} (MPa)	K_{Ic}^J (MPa m$^{1/2}$)	Critical plastic zone radius (mm)	LTR (mm)
883	20.0	0.05	0.093	1080	29.2	0.040	0.120
821	24.8	0.050	0.096	990	35.6	0.071	0.121
780	27.0	0.066	0.101	925	41.0	0.102	0.146
683	33.5	0.127	0.132	828	45.4	0.165	0.158
642	36.0	0.172	0.152	738	51.5	0.267	0.178
587	41.0	0.269	0.172	666	56.7	0.381	0.187
555	42.7	0.304	0.183	597	64.0	0.632	0.209
486	50.0	0.711	0.210	559	74.5	0.965	0.330

at different yield strength levels and compared with the ρ_L values in Table III. It may be seen from Table III that the plastic zone radius is of the same order as the limiting crack tip radius for cleavage induced fracture. At an intermediate strength level, the agreement between the two is fairly good. In low yield strength regime fracture initiates partially by non-cleavage mode, which is considered to be instrumental for a larger increase in the plastic zone size. However, the relation between the plastic zone radius and the limiting crack tip radius requires further investigation.

5. Conclusions

From the present investigation following conclusions are made.

1. The blunting crack tip radius, obtained from the CTOD value at the instant of cleavage fracture initiation, is found to be uniquely related with the limiting crack tip radius for the structural steels at different yield strength levels.

2. Blunting as well as the limiting crack tip radius are dependent on the yield strength as per Equations 9, 10 and 11 for cleavage fracture.

3. The limiting crack tip radius does not appear to be related to the grain diameter or interinclusion spacing and appears to be an order larger than either of them.

4. The limiting crack tip radius is of the order of the radius of plastic zone size. This requires further confirmation.

Acknowledgement

The author is grateful to Professor S. Banerjee for useful discussion and keen interest in the work.

References

1. G. IRWIN, *Appl. Mater. Res.* **3** (1964) 2.
2. J. H. MULHERIN, D. F. ARMIENTO and H. MARKUS, *J. Basic Eng.* (1964) 709.
3. T. R. WILSHAW, C. A. RAU and A. S. TETELMAN, *Eng. Fracture Mech.* **1** (1968) 191.
4. G. OATES, *J. Iron Steel Inst.* **205** (1967) 41.
5. J. R. RICE and M. A. JOHNSON, "Inelastic Behaviour of Solids", edited by M. F. Kanninen *et al.* (McGraw Hill, New York, 1970).
6. J. P. TANAKA, C. A. PAMBILLO and J. R. LOW, ASTM STP 463 (American Society for Testing and Materials, Philadelphia, 1970) p. 191.
7. R. K. PANDEY and S. BANERJEE, *Eng. Fract. Mech.* **5** (1973) 965.
8. R. W. NICHOLS, F. M. BURDEKIN, A. COWAN, D. ELLIOT and T. INGHAM, "Practical Fracture Mechanics for Structural Steel", (Chapman and Hall, London 1969).
9. C. C. VEERMAN and T. MULLER, *Eng. Fract. Mech.* **4** (1972) 25.
10. J. MALKIN and A. S. TETELMAN, *ibid.* **3** (1971) 151.
11. J. A. BEGLEY and J. D. LANDES, ASTM STP 514 (American Society for Testing and Materials, Philadelphia, 1972).
12. R. K. PANDAY and S. BANERJEE, *Trans. Ind. Inst. Met.* **30** (5) (1977) 301.
13. G. A. CLARK, W. R. ANDREWS, J. A. BEGLEY, J. K. DONALD, G. T. EMBLEY, J. D. LANDES, D. E. McCABE and J. H. UNDERWOOD, *J. Test. Eval.* **7** (1) (1979) 49.
14. J. D. LANDES and J. A. BEGLEY, ASTM STP 560 (American Society for Testing and Materials, Philadelphia, 1974) p. 170.
15. A. S. TETELMAN and A. J. McEVILY, "Fracture of Structural Materials" (Wiley, New York, 1967).
16. R. K. PANDEY, J. D. HARIDAS and S. BANERJEE, *Eng. Fract. Mech.* **6** (1974) 105.
17. A. H. COTTRELL, "The Mechanical Properties of Matter" (Wiley, New York, 1963).
18. J. F. KNOTT, "Fundamentals of Fracture Mechanics" (Butterworths, London, 1973).
19. G. R. IRWIN and F. A. McCLINTOCK, ASTM STP 381 (American Society for Testing and Materials, Philadelphia, 1965).

Received 19 January
and accepted 24 June 1983